

**AFRL-IF-WP-TP-2005-500**

**EVOLVING NOVEL COEFFICIENT SETS  
FOR OPTIMIZED RECONSTRUCTION  
OF QUANTIZED ONE-DIMENSIONAL  
(1-D) AND TWO-DIMENSIONAL (2-D)  
SIGNALS**

**2004 Visiting Faculty Research Program (VFRP)  
In-House Work at AFRL/IFTA**

**Pat Marshall  
Frank Moore**



**SEPTEMBER 2004**

**Approved for public release; distribution is unlimited.**

**STINFO FINAL REPORT**

**INFORMATION DIRECTORATE  
AIR FORCE RESEARCH LABORATORY  
AIR FORCE MATERIEL COMMAND  
WRIGHT-PATTERSON AIR FORCE BASE, OH 45433-7334**

## NOTICE

Using Government drawings, specifications, or other data included in this document for any purpose other than Government procurement does not in any way obligate the U.S. Government. The fact that the Government formulated or supplied the drawings, specifications, or other data does not license the holder or any other person or corporation; or convey any rights or permission to manufacture, use, or sell any patented invention that may relate to them.

This report was cleared for public release by the Air Force Research Laboratory Wright Site Public Affairs Office (AFRL/WS) and is releasable to the National Technical Information Service (NTIS). It will be available to the general public, including foreign nationals.

THIS TECHNICAL REPORT IS APPROVED FOR PUBLICATION.

/s/

---

PAT MARSHALL, Project Engineer/Team Leader  
Embedded Information Systems Branch  
Advanced Computing Division  
Information Directorate

/s/

---

JAMES WILLIAMSON, Chief  
Embedded Information Systems Branch  
Advanced Computing Division  
Information Directorate

This report is published in the interest of scientific and technical information exchange and its publication does not constitute the Government's approval or disapproval of its ideas or findings.

REPORT DOCUMENTATION PAGE				Form Approved OMB No. 0704-0188	
<p>The public reporting burden for this collection of information is estimated to average 1 hour per response, including the time for reviewing instructions, searching existing data sources, searching existing data sources, gathering and maintaining the data needed, and completing and reviewing the collection of information. Send comments regarding this burden estimate or any other aspect of this collection of information, including suggestions for reducing this burden, to Department of Defense, Washington Headquarters Services, Directorate for Information Operations and Reports (0704-0188), 1215 Jefferson Davis Highway, Suite 1204, Arlington, VA 22202-4302. Respondents should be aware that notwithstanding any other provision of law, no person shall be subject to any penalty for failing to comply with a collection of information if it does not display a currently valid OMB control number. <b>PLEASE DO NOT RETURN YOUR FORM TO THE ABOVE ADDRESS.</b></p>					
1. REPORT DATE (DD-MM-YY) September 2004		2. REPORT TYPE Final		3. DATES COVERED (From - To) 06/22/2004 – 08/31/2004	
4. TITLE AND SUBTITLE EVOLVING NOVEL COEFFICIENT SETS FOR OPTIMIZED RECONSTRUCTION OF QUANTIZED ONE-DIMENSIONAL (1-D) AND TWO- DIMENSIONAL (2-D) SIGNALS 2004 Visiting Faculty Research Program (VFRP) In-House Work at AFRL/IFTA				5a. CONTRACT NUMBER In-house	
				5b. GRANT NUMBER	
				5c. PROGRAM ELEMENT NUMBER 62702F	
6. AUTHOR(S) Pat Marshall (AFRL/IFTA) Frank Moore (University of Alaska, Anchorage)				5d. PROJECT NUMBER SUNY	
				5e. TASK NUMBER 03	
				5f. WORK UNIT NUMBER IT	
7. PERFORMING ORGANIZATION NAME(S) AND ADDRESS(ES) <div style="display: flex; justify-content: space-between;"> <div style="width: 45%;"> Embedded Information Systems Branch (AFRL/IFTA)  Advanced Computing Division  Information Technology Directorate  Air Force Research Laboratory, Air Force Materiel Command  Wright-Patterson Air Force Base, OH 45433-7334 </div> <div style="width: 45%;"> University of Alaska, Anchorage  Dept. of Mathematical Sciences  CAS 154, 3211 Providence Dr.  Anchorage, AK 99508 </div> </div>				8. PERFORMING ORGANIZATION REPORT NUMBER AFRL-IF-WP-TP-2005-500	
9. SPONSORING/MONITORING AGENCY NAME(S) AND ADDRESS(ES) Information Directorate Air Force Research Laboratory Air Force Materiel Command Wright-Patterson AFB, OH 45433-7334				10. SPONSORING/MONITORING AGENCY ACRONYM(S) AFRL/IFTA	
				11. SPONSORING/MONITORING AGENCY REPORT NUMBER(S) AFRL-IF-WP-TP-2005-500	
12. DISTRIBUTION/AVAILABILITY STATEMENT Approved for public release; distribution is unlimited.					
13. SUPPLEMENTARY NOTES Report contains color.					
14. ABSTRACT This paper describes a genetic algorithm that evolves optimized sets of coefficients for signal reconstruction under lossy conditions due to quantization. Beginning with a population of mutated copies of the set of coefficients describing a wavelet-based inverse transform, our genetic algorithm systemically evolves a new set of coefficients that significantly reduces mean squared error (relative to the performance of the selected wavelet) for various classes of one- and two-dimensional signals.					
15. SUBJECT TERMS Genetic algorithms, discrete wavelet algorithms, quantization noise					
16. SECURITY CLASSIFICATION OF:			17. LIMITATION OF ABSTRACT: SAR	18. NUMBER OF PAGES 18	19a. NAME OF RESPONSIBLE PERSON (Monitor) Pat Marshall 19b. TELEPHONE NUMBER (Include Area Code) (937) 255-6548 x3586
a. REPORT Unclassified	b. ABSTRACT Unclassified	c. THIS PAGE Unclassified			

# EVOLVING NOVEL COEFFICIENT SETS FOR OPTIMIZED RECONSTRUCTION OF QUANTIZED ONE-DIMENSIONAL (1-D) AND TWO-DIMENSIONAL (2-D) SIGNALS

**Abstract.** This paper describes a genetic algorithm that evolves optimized sets of coefficients for signal reconstruction under lossy conditions due to quantization. Beginning with a population of mutated copies of the set of coefficients describing a wavelet-based inverse transform, our genetic algorithm systemically evolves a new set of coefficients that significantly reduces mean squared error (relative to the performance of the selected wavelet) for various classes of 1-D and 2-D signals.

## 1 INTRODUCTION

Wavelets [1] are commonly used to solve problems drawn from a wide range of application areas. Wavelet transforms associated with orthonormal, compactly supported wavelets [2] and biorthogonal wavelets [3] have been shown to achieve signal compression ratios as high as 10:1, 50:1, and even 100:1 without significant information loss. In these cases, the corresponding inverse wavelet transforms are capable of reconstructing very close approximations of the original signal.

For many practical problems, however, it becomes necessary to represent a given signal using a smaller range of possible values. For example, telephone signals (for which speed of transmission is most important) are represented by as few as 8 bits, while music signals (which require higher signal fidelity) are typically represented by 16-bit values. *Quantization* [4] is the process of mapping signals to a smaller number of bits. Figure 1 illustrates the process of reconstructing quantized 1-D signals. A 2-D transform is accomplished by performing a 1-D transform on each row of the image, followed by a 1-D transform on each column.

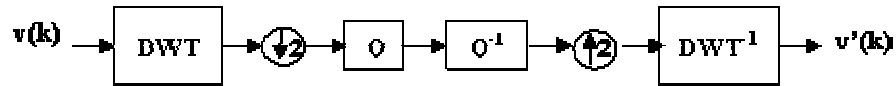


**Figure 1. 1-D Reconstruction Discrete Wavelet Transform (DWT) Filter with Quantization**

Errors introduced into the transformed signal via quantization may have an unacceptably adverse effect upon the quality of the signal when it is subsequently reconstructed via the wavelet inverse transform. A growing amount of empirical evidence (e.g., [5]) suggests that nontraditional inverse transformations may do a better job of compensating for the negative effects of quantization, resulting in higher fidelity signal reconstruction. In particular, recent studies suggest that the use of adaptive ([6], [7]) and/or nonstandard [8]

filters may significantly reduce errors for specific classes of signals, which typically share spatial domain characteristics.

## 2 METHODOLOGY

Genetic algorithms (GAs) are optimization techniques inspired by Darwinian evolution. GAs [9] have been successfully applied to an ever-increasing number of difficult and interesting optimization problems. The goal of this investigation was to develop a GA capable of automatically modifying the coefficient sets describing wavelet inverse transform functions [10] to evolve novel inverse transforms exhibiting significantly improved performance for a given class of signals [11]. In particular, our GA automatically compensated for errors introduced into the original signal by quantization. Performance may be measured in many ways [12]; for this study, performance equaled the mean squared error (MSE) in the reconstructed signal.

Figure 2 illustrates our GA-based inverse transform optimization process. The best-of-run inverse transform coefficients produced by the GA are used to replace the  $DWT^{-1}$  shown in Figure 1. To improve upon wavelet-based techniques, our GA had to evolve optimized inverse transform coefficients that significantly reduced the aggregate MSE in each reconstructed signal  $v'(k)$ .

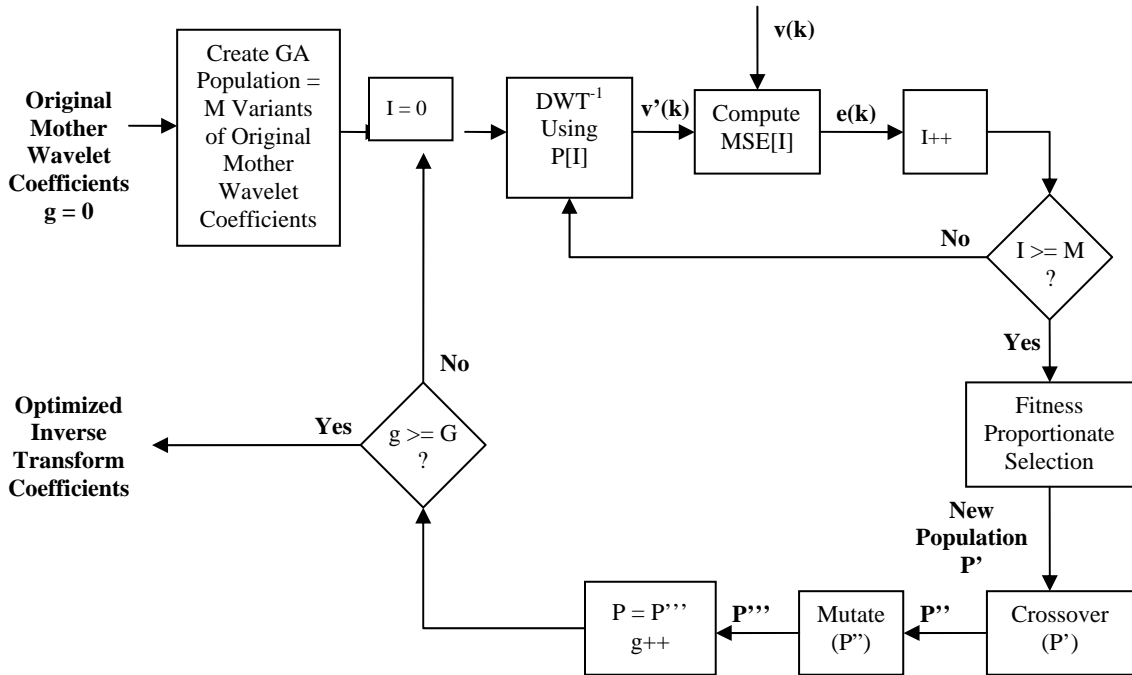


Figure 2. Detailed GA for Optimization of Coefficients for Inverse Transforms

### 3 TEST RESULTS

We conducted a series of tests to demonstrate the performance of GA-evolved transforms relative to that of the *Daubechies-4* (Daub4) wavelet inverse transform [10], which may be described by the following sets of floating-point coefficients:

$$\begin{aligned}h2 &= \{0.4830, 0.8365, 0.2241, -0.1294\} \\g2 &= \{-0.1294, -0.2241, 0.8365, -0.4830\}\end{aligned}$$

Each test was characterized by a particular combination of the following parameters:

1. **SIGNAL CLASS.** Each test trained our GA using signals drawn from a particular class. One-dimensional signal classes used in this study included ramp functions, sine waves, and random signals. Additional tests were performed using 2-D photographic images. These classes were chosen due to their relevance to real-world applications.
2. **G** specified the (maximum) number of generations executed by our GA. Preliminary experiments indicated that a large G value was necessary to allow our GA to progress toward a globally optimized solution. For each of the 1-D signal tests performed for this study,  $G = 10,000$ . Since the amount of data processed during the 2-D tests was an order of magnitude greater than for 1-D signals, it became necessary to use only  $G = 500$  generations.
3. **M** specified the population size (i.e., the number of candidate solutions in each generation). For each of the tests performed for this study,  $M = 500$ .
4. **P<sub>C</sub>** specified the percentage of individuals in the next generation subjected to the crossover operator. Preliminary experiments demonstrated the benefits of a high crossover rate; for this reason, each of the tests performed for this study used  $P_C = 100 \text{ percent} * (M-1)/M = 99.8 \text{ percent}$ .
5. **P<sub>M</sub>** specified the probability of mutation, as described below.
6. **N** specified the size of the training population (i.e., the number of signals used to train our GA).

Our GA copied the best individual from the current generation into position 0 of the next generation; this individual was not subject to subsequent crossover or mutation. Our GA selected the remaining  $M-1$  individuals from the current generation via tournaments of three randomly selected individuals. These individuals were then probabilistically subjected to the crossover operator according to  $P_C$ . Finally, each coefficient of these  $M-1$  individuals was subjected to the mutation operator with probability  $P_M$ . Our GA initialized  $P_M$  to 2 percent. If the current generation failed to produce a new globally optimal set of coefficients, our GA automatically increased  $P_M$  by 1 percent, up to a maximum of 20 percent; otherwise, our GA reset  $P_M$  to 2 percent.

#### 3.1 Class 1: Ramp Signals

One-dimensional ramp signals are important for a variety of applications. For example, ramp response signals provide information about the size, shape, and orientation of dielectric targets [13]. Tests 1, 2, and 3 populated the training set with  $N$  ramp signals,

each of which contained 50 values. For each signal, our GA initialized the starting value  $\alpha$  to a randomly selected integer between 255 and 511; set the stopping value  $\omega$  to  $\alpha/2$ ; and used the following algorithm to determine the remaining values:

```

if ( $v[i] == \omega$ )
     $v[i+1] = \alpha$ ;
else
     $v[i+1] = v[i] - 1$ ;

```

Our GA initialized each of the  $g_2$  and  $h_2$  coefficients for the inverse transforms in generation 0 to a randomly mutated version of the corresponding coefficient from the Daub4 wavelet.

Table 1 summarizes the performance (as measured by the total MSE for  $N$  reconstructed signals) of each novel inverse transform described by a GA-evolved best-of-run coefficient set, relative to that of the Daub4 wavelet.

**Table 1. Ramp Signal Test Results**

<u>Test</u>	<u>N</u>	<u>MSE (Daub4)</u>	<u>MSE (evolved)</u>	<u>% Improvement</u>
1	100	5505.1	4838.9	12.1
2	25	1376.0	1215.0	11.7
3	10	552.4	522.9	5.35

These tests evolved the following sets of coefficients for the optimized inverse transform:

Test 1:  $h_2 = \{0.3167, 0.8038, 0.3911, -0.0979\}$   
 $g_2 = \{-0.1700, -0.6120, 0.9813, -0.3859\}$   
Test 2:  $h_2 = \{0.3203, 0.8113, 0.3875, -0.1054\}$   
 $g_2 = \{0.1493, -0.0852, -0.4700, 0.2132\}$   
Test 3:  $h_2 = \{0.4053, 0.8110, 0.3024, -0.1052\}$   
 $g_2 = \{-0.0705, 0.1193, -0.8903, 0.2180\}$

The results of these tests demonstrate the following key points:

- 1) Novel inverse transforms exist that outperform the Daub4 wavelet inverse transform for reconstructing arbitrary ramp signals that have been subjected to lossy quantization operations.
- 2) Our GA is capable of automatically optimizing coefficient sets for these novel inverse transforms.
- 3) Training on a larger population of ramp signals allows our GA to evolve solutions that exhibit better generalization properties.

### 3.2 Class 2: Sine Waves

The detection of periodic behavior in 1-D signals continues to be a research topic of considerable importance [14]. Tests 4 through 12 populated the training set with various types of sine waves. Each wave was characterized by the following parameters:

**g** = gain  
**f** = frequency  
**d** = offset.

For these tests, each vector **v** consisted of 50 sampled values defined as follows:

```
for (i = 0; i < 50; i++)  
    v[i] = g * sin (2πf * i) + d;
```

Table 2 summarizes the performance of GA-evolved best-of-run coefficient sets optimized under conditions described by various combinations of frequency (**f**), gain (**g**), and offset (**d**), relative to that of the Daub4 wavelet described above.

**Table 2. Sine Wave Test Results**

<u>Test</u>	<u>N</u>	<u><b>g</b></u>	<u><b>d</b></u>	<u><b>f</b></u>	<u>MSE (Daub4)</u>	<u>MSE (evolved)</u>	<u>% Improvement</u>
4	100	128	256	0...999	1096.19	86.69	92.1
5	25	128	256	0...999	269.00	20.18	92.5
6	10	128	256	0...999	124.55	3.55	97.2
7	100	128	0...255	1000	5207.62	5034.13	3.33
8	25	128	0...255	1000	1203.68	1182.69	1.74
9	10	128	0...255	1000	403.67	397.82	1.45
10	100	0...127	256	1000	1123.89	88.19	92.2
11	25	0...127	256	1000	274.49	24.90	90.9
12	10	0...127	256	1000	108.94	10.30	90.6



These tests evolved the following sets of coefficients for optimized inverse transforms:

Test 4:  $h2 = \{0.4875, 0.8279, 0.2109, -0.1294\}$   
           $g2 = \{-0.1280, -0.2430, -0.6366, -0.4881\}$   
Test 5:  $h2 = \{0.4876, 0.8280, 0.2109, -0.1294\}$   
           $g2 = \{0.1156, 0.2664, 0.9523, 0.3452\}$   
Test 6:  $h2 = \{0.4780, 0.8282, 0.2196, -0.1305\}$   
           $g2 = \{-0.1398, 0.2286, 0.8616, 0.4919\}$   
Test 7:  $h2 = \{0.4447, 0.7768, 0.2569, -0.0747\}$   
           $g2 = \{-0.1050, -0.3507, -0.2918, 0.3030\}$   
Test 8:  $h2 = \{0.4448, 0.7849, 0.2592, -0.0805\}$   
           $g2 = \{0.0752, -0.2607, -0.7085, -0.6749\}$   
Test 9:  $h2 = \{0.4927, 0.8024, 0.2175, -0.0920\}$   
           $g2 = \{-0.0649, 0.5076, -1.0222, 0.2395\}$   
Test 10:  $h2 = \{0.4877, 0.8278, 0.2106, -0.1294\}$   
           $g2 = \{-0.1631, -0.2723, -0.9434, 0.5711\}$   
Test 11:  $h2 = \{0.4876, 0.8280, 0.2108, -0.1294\}$   
           $g2 = \{0.1542, -0.2062, -0.7879, 0.4552\}$   
Test 12:  $h2 = \{0.4777, 0.8279, 0.2208, -0.1293\}$   
           $g2 = \{0.1337, -0.2792, 0.7655, -0.2608\}$

Tests 4, 5, and 6 demonstrated that our GA was capable of identifying coefficients for inverse transforms that significantly outperformed the Daub4 inverse transform for the task of reconstructing sine waves characterized by different  $f$  values. For this signal class, GA-optimized transforms were capable of reducing MSE in the reconstructed signal by a factor of 12 or more. It is interesting to note that, while the magnitude of the four coefficients comprising set  $h2$  were virtually identical, the four coefficients from set  $g2$  exhibited far greater variation, even to the extent of having opposite signs.

Tests 7, 8, and 9 showed that, when the training set consisted of sine waves that differed only according to the offset  $d$ , little advantage was to be gained from evolving novel coefficients for inverse transforms. For these three tests, the performance of the inverse transforms described by the evolved coefficient sets improved upon that of the Daub4 inverse transform by an average of only 2.17 percent. These tests also showed much greater variation in the magnitude of  $g2$  coefficients than  $h2$  coefficients, as well as differences in the sign of those coefficients.

Tests 10, 11, and 12 demonstrated our GA's ability to evolve coefficients for inverse transforms that significantly outperformed the Daub4 inverse transform for the task of reconstructing sine waves that differed only in the gain value  $g$ . For this class of signal, GA-optimized inverse transforms were capable of reducing MSE in the reconstructed signal by a factor of 11 or more. As with previous tests, these results showed greater variation in the magnitude of  $g2$  coefficients; indeed, the  $h2$  coefficients evolved during these three tests were identical in sign and virtually identical in magnitude, while the  $g2$  coefficients varied in both sign and magnitude.

### 3.3 Class 3: Random Functions

Tests 13, 14, and 15 populated the training set with one-dimensional vectors  $\mathbf{v}$  consisting of 50 random values between 0 and 255 (inclusive). Table 3 summarizes test results under a variety of conditions, relative to the MSE produced by the Daub4 inverse wavelet.

**Table 3. Test Results for Random Signals**

<u>Test</u>	<u>N</u>	<u>MSE (Daub4)</u>	<u>MSE (evolved)</u>	<u>% Improvement</u>
13	100	12680.4	12529.2	1.19
14	25	3271.3	3230.7	1.24
15	10	1390.0	1333.7	1.04

These tests evolved the following sets of optimized inverse transform coefficients:

Test 13:  $h2 = \{0.4781, 0.8248, 0.2285, -0.1177\}$   
           $g2 = \{-0.1279, -0.2174, 0.8248, -0.4728\}$   
Test 14:  $h2 = \{0.4781, 0.8268, 0.2331, -0.1209\}$   
           $g2 = \{-0.1236, -0.2262, 0.8199, -0.4763\}$   
Test 15:  $h2 = \{0.4864, 0.8282, 0.2234, -0.1192\}$   
           $g2 = \{-0.1363, -0.2135, 0.8263, -0.4734\}$

The average performance (in terms of MSE) of the inverse transforms described by our GA-evolved coefficient sets from tests 13, 14, and 15 was only 1.16 percent better than that of the Daub4 wavelet inverse transform. This advantage remained nearly negligible as the number of random signals in the training population increased. Truly random signals exhibit no particular pattern; for this reason, our GA was unable to find and exploit information common to all of the signals in the training set.

### 3.4 Class 4: Images

The goal of Tests 16 and 17 was to determine whether the GA-based methodology established by Tests 1-15 could be used to evolve a transform that outperformed the Daub4 wavelet when reconstructing *2-D images* previously subjected to quantization error. Test 16 used a training set populated with  $N$  portrait-like photographs similar to the image shown in Figure 3, while Test 17 used landscape-like photographs similar to those shown in Figure 4. Each photographic image consisted of a 512- by 512-array of red, green, and blue (RGB) color pixels. Prior to evolution, our GA transformed each image from the training set to the corresponding signal in the luminance (YUV) domain. Each test used a quantization step of 64 (in effect, discarding the information contained in the six least significant bits of each value).

The results of Tests 16 and 17 are summarized in Table 4. These results clearly demonstrate that our GA was capable of evolving a best-of-run transform whose

performance, in terms of reduced total MSE over a class of images, measurably improved upon that of the Daub4 wavelet.

**Table 4. Test Results for 2-D Images**

<u>Test</u>	<u>N</u>	<u>MSE (Daub4)</u>	<u>MSE (evolved)</u>	<u>% Improvement</u>
16	5 (barb, baboon, lenna, susie, zelda)	2.30381e+08	2.18978e+08	4.95
17	5 (airplane, boat, fruits, goldhill, park)	1.85457e+08	1.78302e+08	3.86



**Figure 3. A Typical Portrait-like Photographic Image (“barb.bmp”) from Test 16**



**Figure 4. A Typical Landscape-like Photographic Image (“goldhill.bmp”) from Test 17**

These tests evolved the following sets of coefficients for optimized inverse transforms:

$$\begin{aligned} \text{Test 16: } h_2 &= \{0.4686, 0.8035, 0.2378, -0.1021\} \\ g_2 &= \{-0.2084, -0.1461, 0.7251, -0.3935\} \\ \text{Test 17: } h_2 &= \{0.4637, 0.8116, 0.2449, -0.1095\} \\ g_2 &= \{-0.1680, -0.1644, 0.7555, -0.3732\} \end{aligned}$$

Considerable computational resources were necessary to complete each 2-D run. For example, Test 17 required 46 hours, 53 minutes, 59 seconds of wall clock time on a high-end dedicated PC. Access to supercomputers would allow future tests to use much larger populations (e.g.,  $M = 10,000$ ) over many more generations (e.g.,  $G = 5,000$ ), possibly evolving inverse transforms that exhibit substantially better reconstruction properties than those described above.

## 4 CONCLUSIONS

Collectively, the results of this study suggested that the number of coefficient sets capable of producing high-fidelity signal reconstructions under lossy conditions may be much larger than previously believed. The novel coefficient sets evolved during this study violated wavelet properties required for perfect reconstruction, such as invertibility

and nonredundancy [15]. Nevertheless, the corresponding inverse transforms consistently outperformed the Daub4 inverse transform, often producing significantly higher fidelity reconstructions of periodic signals and images, as measured by the percentage reduction in the MSE of each reconstructed signal. The results of this study strongly encouraged the identification and use of evolved inverse transforms for signal reconstruction under lossy conditions. In particular, our results conclusively demonstrated our GA's ability to automatically identify novel sets of coefficients for inverse transforms that successfully reconstruct various classes of periodic signals and images under lossy conditions subject to quantization.

Our research will continue with significantly larger tests for multidimensional signals and will include a rigorous mathematic analysis of our findings.

## REFERENCES

- [1] Walker, J. S., 1999. *A Primer on Wavelets and Their Scientific Applications*, CRC Press.
- [2] Daubechies, I., 1988. Orthonormal Bases of Compactly Supported Wavelets, *Communications on Pure and Applied Mathematics*, 41: 909-996.
- [3] Cohen, A., I. Daubechies, and J. C. Feauveau, 1992. Biorthogonal Bases of Compactly Supported Wavelets, *Communications on Pure and Applied Mathematics*, 45: 485-560.
- [4] Mallat, S., 1998. *A Wavelet Tour of Signal Processing*, Academic Press.
- [5] Saha, S. and R. Vemuri, 1999. Adaptive Wavelet Filters in Image Coders – How Important Are They?, *IECON'99 Proceedings: The 25th Annual Conference of the IEEE Industrial Electronics Society*, 2: 559-564, IEEE Industrial Electronics Society.
- [6] Claypoole, R. L., R. G. Baraniuk, and R. D. Nowak, 1999. Adaptive Wavelet Transforms via Lifting, Technical Report 9304, Rice University.
- [7] Le Pennec, E. and S. Mallat, 2000. Image Compression with Geometrical Wavelets, *IEEE Conference on Image Processing*, IEEE Signal Processing Society.
- [8] Saha, S. and R. Vemuri, 2000. Analysis-based Adaptive Wavelet Filter Selection in Lossy Image Coding Schemes, *Proceedings: IEEE International Symposium on Circuits and Systems (ISCAS 2000)*, Geneva, Switzerland.
- [9] Goldberg, D. E., 1989. *Genetic Algorithms in Search, Optimization, and Machine Learning*, Addison-Wesley.
- [10] Daubechies, I., 1992. *Ten Lectures on Wavelets*, SIAM.

- [11] Odegard, J., R. Gopinath, and C. Burrus 1994. Design of Linear Phase Cosine Modulated Filter Banks for Subband Image Compression, CML Technical Report, Rice University.
- [12] Lai, Y.-K. and C.-C. J. Kuo, 1997. Image quality measurement using the Haar wavelet, *Wavelet Applications in Signal and Image Processing V*, SPIE.
- [13] Nag, S. K. and L. Peters, Jr. 1998. Ramp Response Signatures for Dielectric Targets, *SPIE Proceedings*, 3392: 703-713, SPIE.
- [14] Venkatachalam, V. and J. Aravena, 1998. Detecting Periodic Behavior in Nonstationary Signals, *IEEE-SP International Symposium on Time-frequency and Time-scale Analysis*, IEEE.
- [15] Piella, G. and H. J. A. M. Heijmans, 2001. Adaptive Lifting Schemes with Perfect Reconstruction, Report PNA-R0104, Centrum voor Wiskunde en Informatica, Stichting Mathematisch Centrum.